Supplementary Information

Tregs delivered post-myocardial infarction adopt an injury-specific phenotype promoting cardiac repair via macrophages in mice

Yasmin K. Alshoubaki[1], Bhavana Nayer[1], Yen-Zhen Lu[1], Ekaterina Salimova[2], Sin Nee Lau[1], Jean L. Tan[1], Daniela Amann-Zalcenstein[3,4], Peter F. Hickey[3,4], Gonzalo del Monte-Nieto[1,5], Ajithkumar Vasanthakumar[6,7,8], and Mikaël M. Martino[1,5*]

[1]European Molecular Biology Laboratory Australia, Australian Regenerative Medicine Institute, Monash University, Melbourne, Australia

[2]Monash Biomedical Imaging, Monash University, Melbourne, Australia

[3]Advanced Genomics Facility, Advanced Technology and Biology Division, The Walter and Eliza Hall Institute of Medical Research, Parkville, Australia

[4]Department of Medical Biology, University of Melbourne, Melbourne, Australia

[5]Victorian Heart Institute, Monash University, Victorian Heart Hospital, Melbourne, Australia

[6]Olivia Newton-John Cancer Research Institute, Heidelberg, Australia

[7]La Trobe University, Bundoora, Australia

[8]Department of Microbiology and Immunology, University of Melbourne, Melbourne, Australia

*Correspondence: mikael.martino@monash.edu

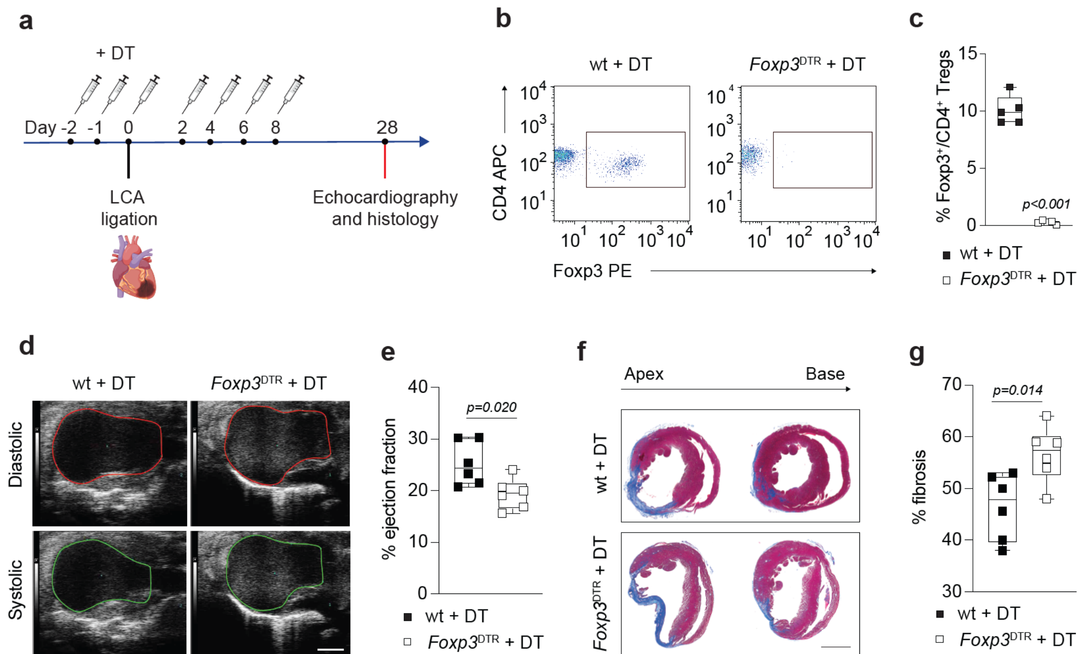

Supplementary Fig. 1 | Treg depletion worsens cardiac repair post-MI. a-g. Wild-type (wt) and *Foxp3*$^{DTR/GFP}$ mice received a diphtheria toxin (DT) treatment to assess the effect of Treg depletion on cardiac function post-MI. The experimental design is shown in (**a**). **b.** Flow cytometry plots showing complete depletion of CD4^{+} Foxp3^{+} cells in the blood 7 days post-MI. **c.** Quantified percentage of the Foxp3^{+} population out of the total CD4^{+} cell population. **d.** Representative parasternal long-axis views of the left ventricles. The red trace is end-diastolic, and the green is end-systolic. Scale bar: 2 mm. **e.** Echocardiographic analysis of the left ventricular ejection fraction expressed as percentage of the left ventricular area in wt and Treg-depleted mice 28 days post-MI (n=6). **g.** Representative histology of whole transverse heart sections from apex to base, 28 days post-MI. Masson's Trichrome staining, scale bar: 2 mm. **g.** Quantification of fibrosis expressed as percentage of the left ventricular area in wt and Treg-depleted mice 28 days post-MI (n=6). For all graphs, boxes show median (centre line) and interquartile range (edges), whiskers show the range of values and dots represent individual data points. Two-tailed Student's t-test was used in (**c**, **e**, **g**). *P* values are indicated. Panel (**a**) created with BioRender.com released under a Creative Commons Attribution-NonCommercial-NoDerivs 4.0 International license (https://creativecommons.org/licenses/by-nc-nd/4.0/deed.en).

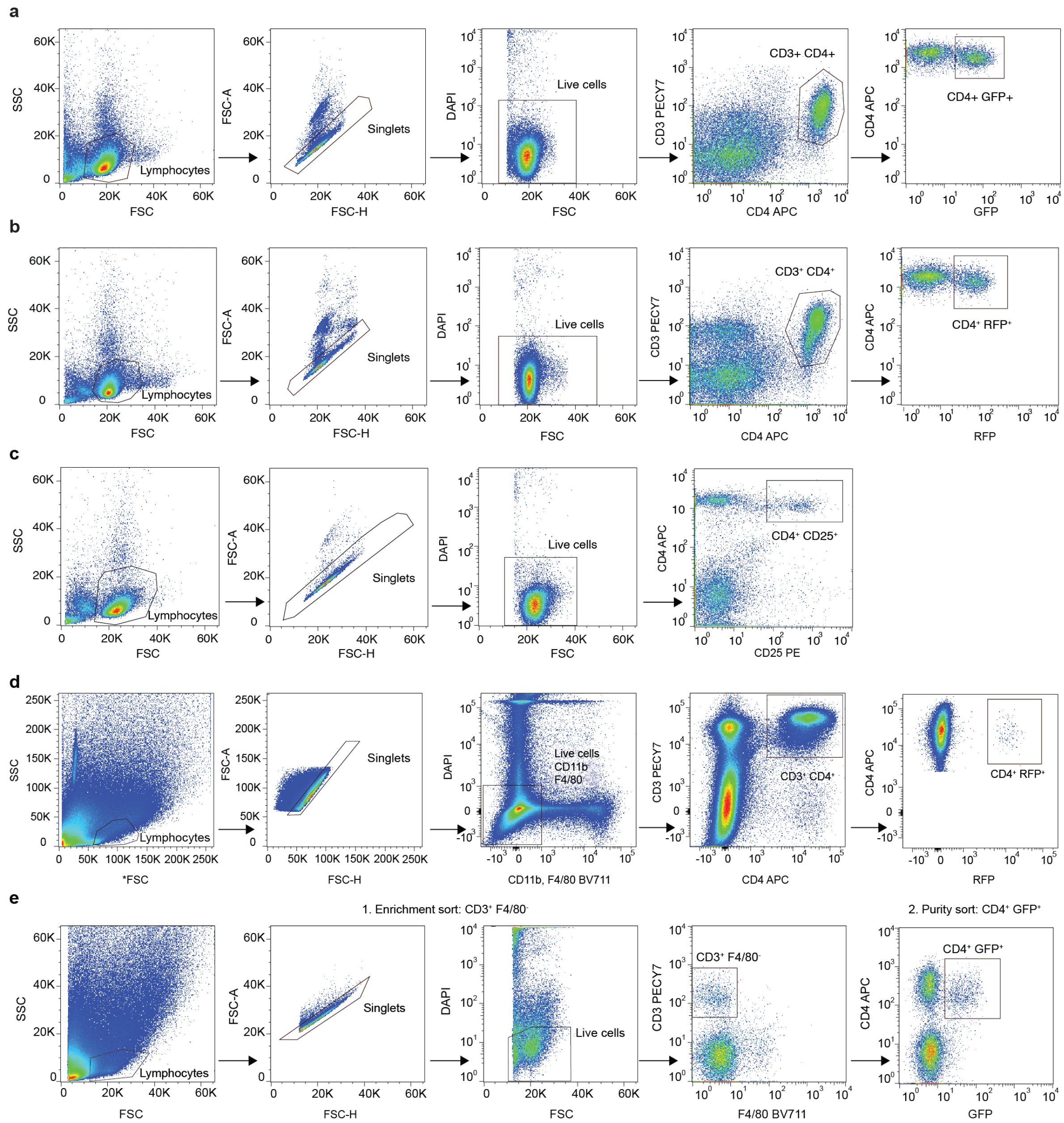

Supplementary Fig. 2 | Sorting of Tregs. a-e. Flow cytometry plots representing the step-by-step gating strategy to obtain a pure population of Tregs. **a.** Tregs were sorted from *Foxp3*$^{DTR/GFP}$ mice spleens. **b.** Tregs were sorted from healthy *Foxp3*$^{IRES\text{-}mRFP}$ mice spleens. **c.** CD4$^+$ CD25$^+$ Tregs were sorted from healthy wild-type mice spleens. **d.** Sorting strategy of RFP$^+$ delivered Tregs from heart, spleen, and MLN on day 3 post-delivery. Exogenous Tregs (CD4$^+$ RFP$^+$) were gated from the CD3$^+$ CD4$^+$ population, following exclusion of myeloid cell populations. **e.** Sorting strategy for endogenous heart Tregs on day 7 post-MI from *Foxp3*$^{DTR/GFP}$ mice. This involves a two-step sort process with an enrichment step CD3$^+$ F4/80$^-$ cells and a purity sort of CD4$^+$ GFP$^+$ cells.

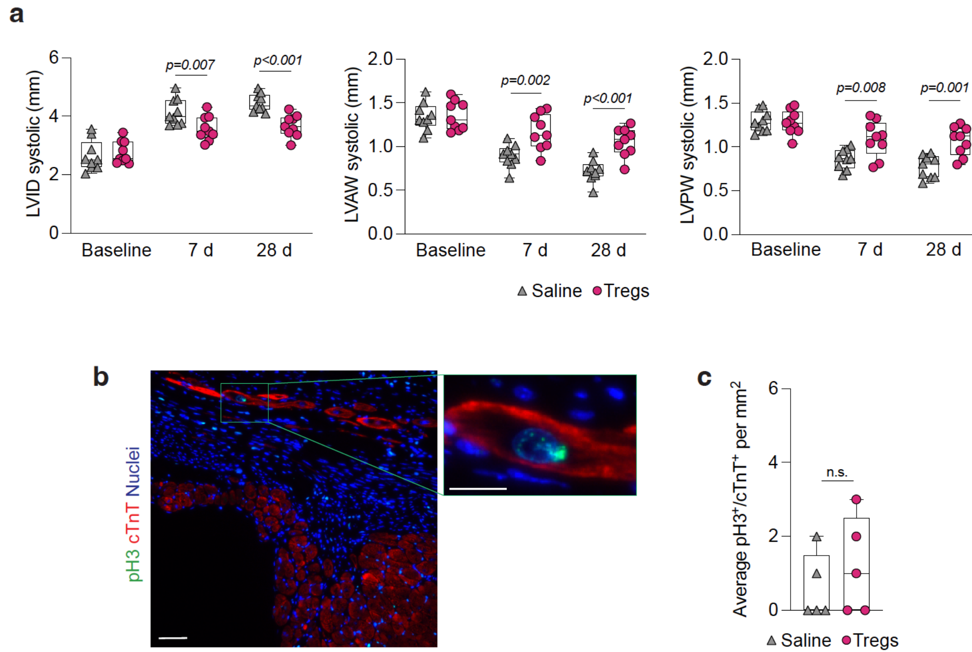

Supplementary Fig. 3 | Additional cardiac function parameters and cardiomyocyte proliferation following Treg treatment. LCA ligation was performed in wild-type (wt) mice. Mice received a systemic injection of saline or Tregs, one day after MI. **a.** Left ventricular systolic internal diameter (LVID), anterior wall (LVAW) and posterior wall (LVPW) thickness (mm) in mice injected with saline or Tregs at baseline, 1- and 4-weeks post-MI (n=9). **b-c.** Sections were stained with Phospho-histone 3 (pH3, in green), cardiac troponin T (cTnT, in red), and nuclei (in blue) to assess cardiomyocyte proliferation seven days post-MI. **b.** Representative field of view showing a cardiomyocyte positive for pH3. Scale bar, 100 µm. **c.** Quantification of the number of $pH3^+/cTnT^+$ cardiomyocytes per mm^2 (n=5). For all graphs, boxes show median (centre line) and interquartile range (edges), whiskers show the range of values and dots represent individual data points. Two-way ANOVA with Bonferroni *post-hoc* test for pair-wise comparisons was used to compare the groups in (**a**). Pairwise comparison was performed with the Two-tailed Student's t-test in (**c**). *P* values are indicated, n.s. indicates non-significant.

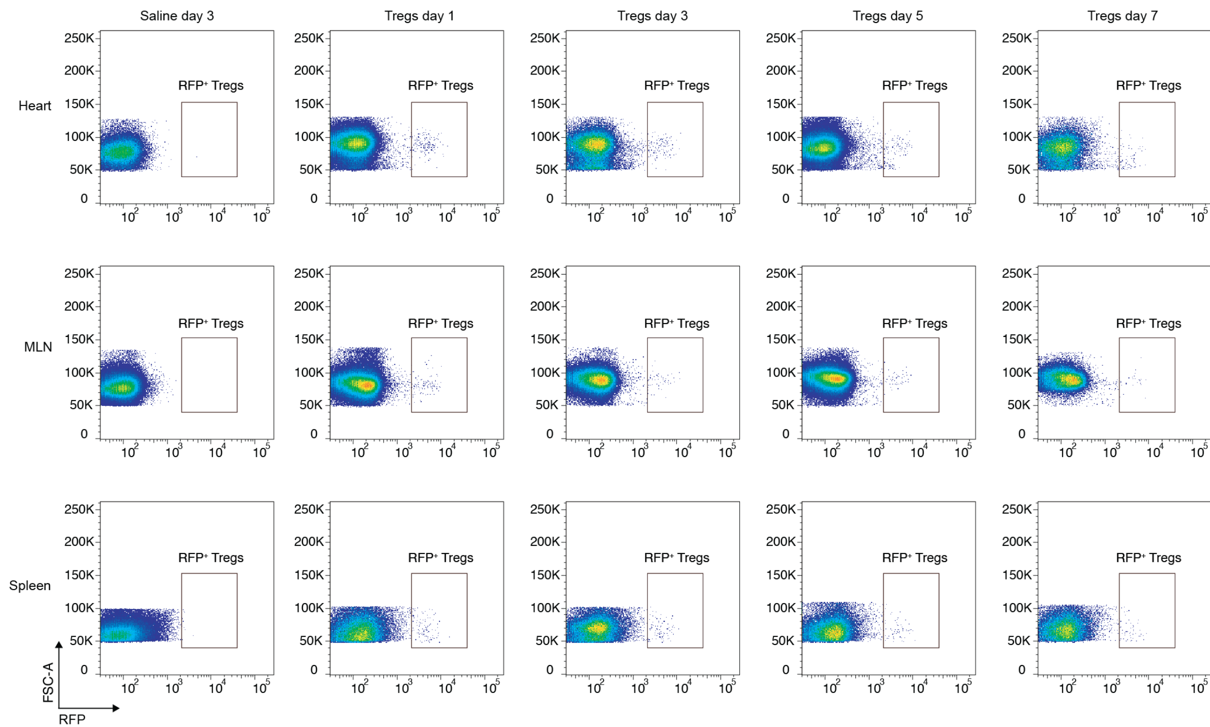

Supplementary Fig. 4 | Delivered RFP$^+$ Tregs home to the heart, MLN, and spleen up to 7 days post-MI. Tregs were sorted from *Foxp3*$^{IRES\text{-}mRFP}$ mouse spleens and delivered into mice one day post-MI. The heart, mediastinal lymph nodes (MLN) and spleen were assessed for the presence for RFP$^+$ Tregs on day 1, 3, 5 and 7 post-delivery. Flow cytometry plots of RFP$^+$ Tregs in the heart, MLN, and spleen in comparison to mice injected with saline control. The RFP population is gated on the CD3$^+$ total population in the respective tissue.

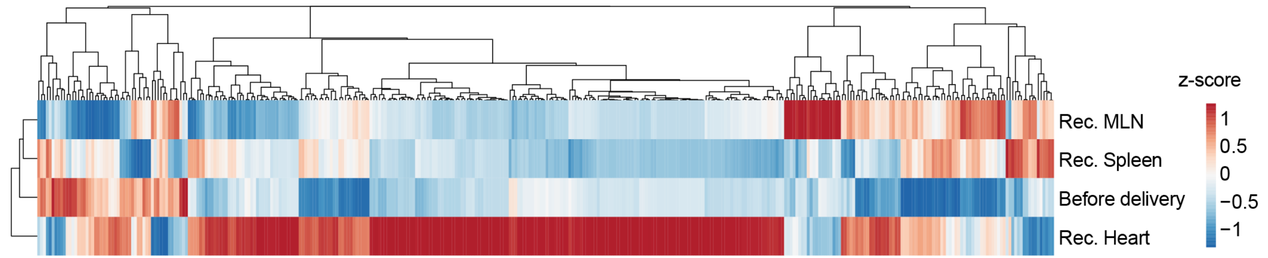

Supplementary Fig. 5 | Overall gene expression profile of exogenous Tregs before delivery and after recovery from heart, MLN and spleen. LCA ligation was performed and mice received a systemic injection of saline or Tregs (from *Foxp3*$^{IRES\text{-}mRFP}$ mice) one day post-MI. Four days post-MI, exogenous Tregs were sorted from the heart, MLN, and spleen and mini-Bulk RNAseq was performed. Hierarchical Clustering Heatmap shows differentially expressed genes (FDR < 0.05) between Tregs before delivery and after being recovered (Rec.) from MLN, spleen and heart (z-scores represent standardised Log_2 CPM values).

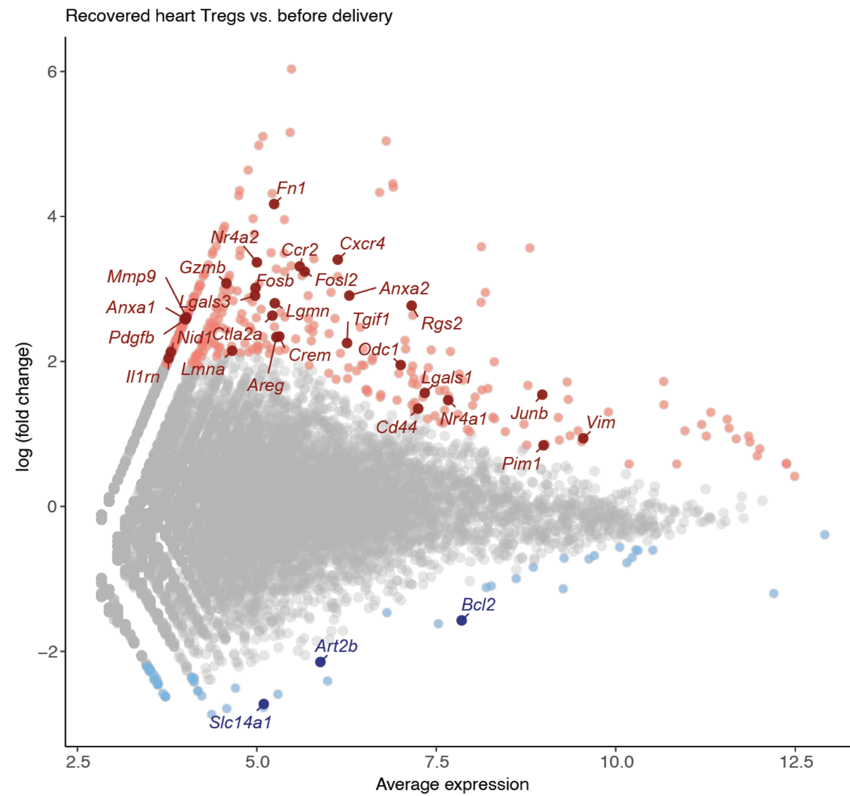

Supplementary Fig. 6 | Global differential expression of exogenous Tregs recovered from the heart vs. Tregs before delivery. LCA ligation was performed and mice received a systemic injection of saline or Tregs (from *Foxp3*$^{IRES\text{-}mRFP}$ mice) one day post-MI. Four days post-MI, exogenous Tregs were sorted and mini-Bulk RNAseq was performed. The MA-plot represents all differentially expressed genes (FDR < 0.05, fold change > |1.5|) with labelled selected genes in exogenous Tregs recovered from the heart vs. before delivery.

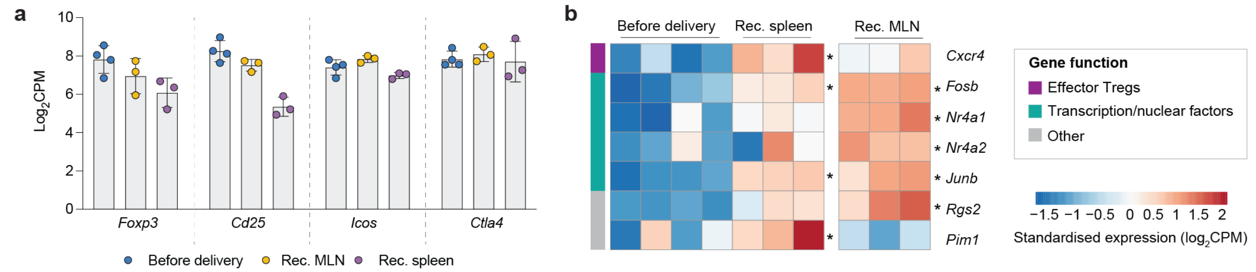

Supplementary Fig. 7 | Gene expression profile of exogenous Tregs recovered from spleen and MLN. LCA ligation was performed and mice received a systemic injection of saline or Tregs (from *Foxp3*$^{IRES\text{-}mRFP}$ mice) one day post-MI. Four days post-MI, exogenous Tregs were sorted from the spleen and MLN, and mini-Bulk RNAseq was performed (Data are presented as mean ± SD, n=4 for saline, n=3 for Tregs). **a.** CPM plots depicting gene expression levels of Treg markers in exogenous Tregs before delivery and exogenous Tregs recovered from the MLN and spleen. **b.** Heat map of selected upregulated and downregulated genes depicting standardised gene expression values in Tregs before delivery and recovered (Rec.) from the MLN and spleen (individual biological replicates are shown). Genes are classified according to main known function with the coloured tab of the heat map. Stars indicate genes that are significantly differentially expressed in spleen or MLN (FDR < 0.05, fold change > |1.5|).

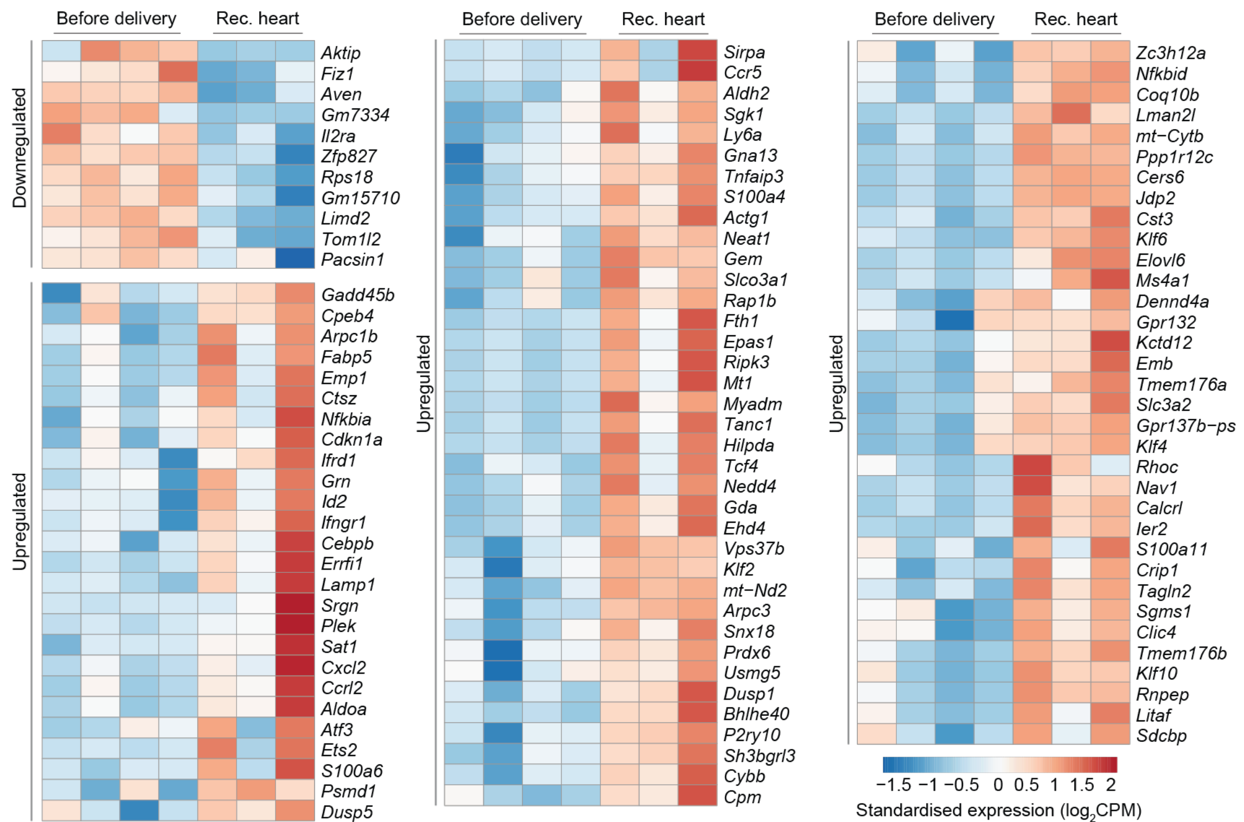

Supplementary Fig. 8 | All additional differentially expressed genes (DEGs) in exogenous Tregs recovered from the heart are common with endogenous heart Tregs. LCA ligation was performed and endogenous heart Tregs were sorted 7 days post-MI for bulk RNA sequencing. For recovery experiments, mice received a systemic injection of saline or Tregs (from *Foxp3*$^{IRES\text{-}mRFP}$ mice) one day post-MI. Four days post-MI, exogenous Tregs were sorted based on RFP expression from the heart and mini-Bulk RNAseq was performed. Heat map depicting standardised gene expression values of DEGs (FDR < 0.05) in exogenous recovered (Rec.) from the heart Tregs vs. Tregs before delivery. Individual biological replicates are shown All these additional DEGs are also shared with endogenous heart Tregs.

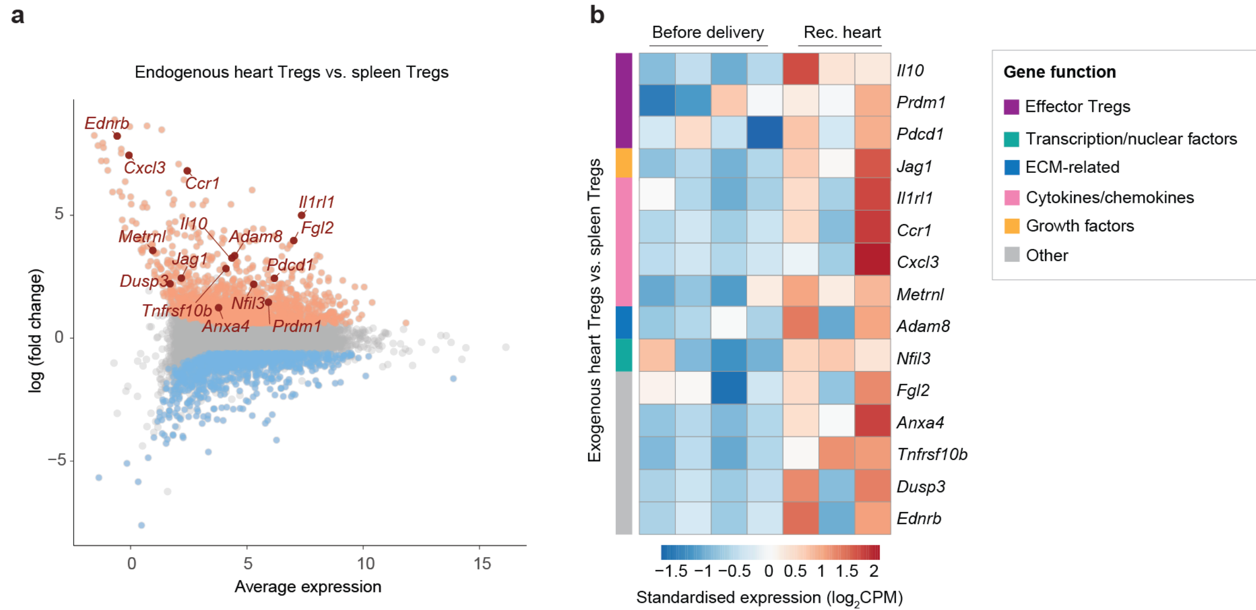

Supplementary Fig. 9 | Additional shared genes that are upregulated in endogenous heart Tregs and highly expressed in exogenous heart Tregs. LCA ligation was performed and endogenous Tregs were sorted 7 days post-MI for bulk RNA sequencing. For recovery experiments, mice received a systemic injection of saline or Tregs (from *Foxp3$^{IRES\text{-}mRFP}$* mice) one day post-MI. Four days post-MI, exogenous Tregs were sorted from the heart and mini-Bulk RNAseq was performed. **a.** MA-plot of differentially expressed genes (FDR < 0.05) in endogenous Tregs sorted from the infarcted heart vs. Tregs from the spleen. **b.** Heat map of the upregulated additional common genes between endogenous heart Tregs and exogenous Tregs depicting standardised gene expression values in Tregs before delivery and Tregs recovered (Rec.) from the heart (individual biological replicates are shown). Fold change > 2. Genes are classified according to main known function with the coloured tab of the heat map.

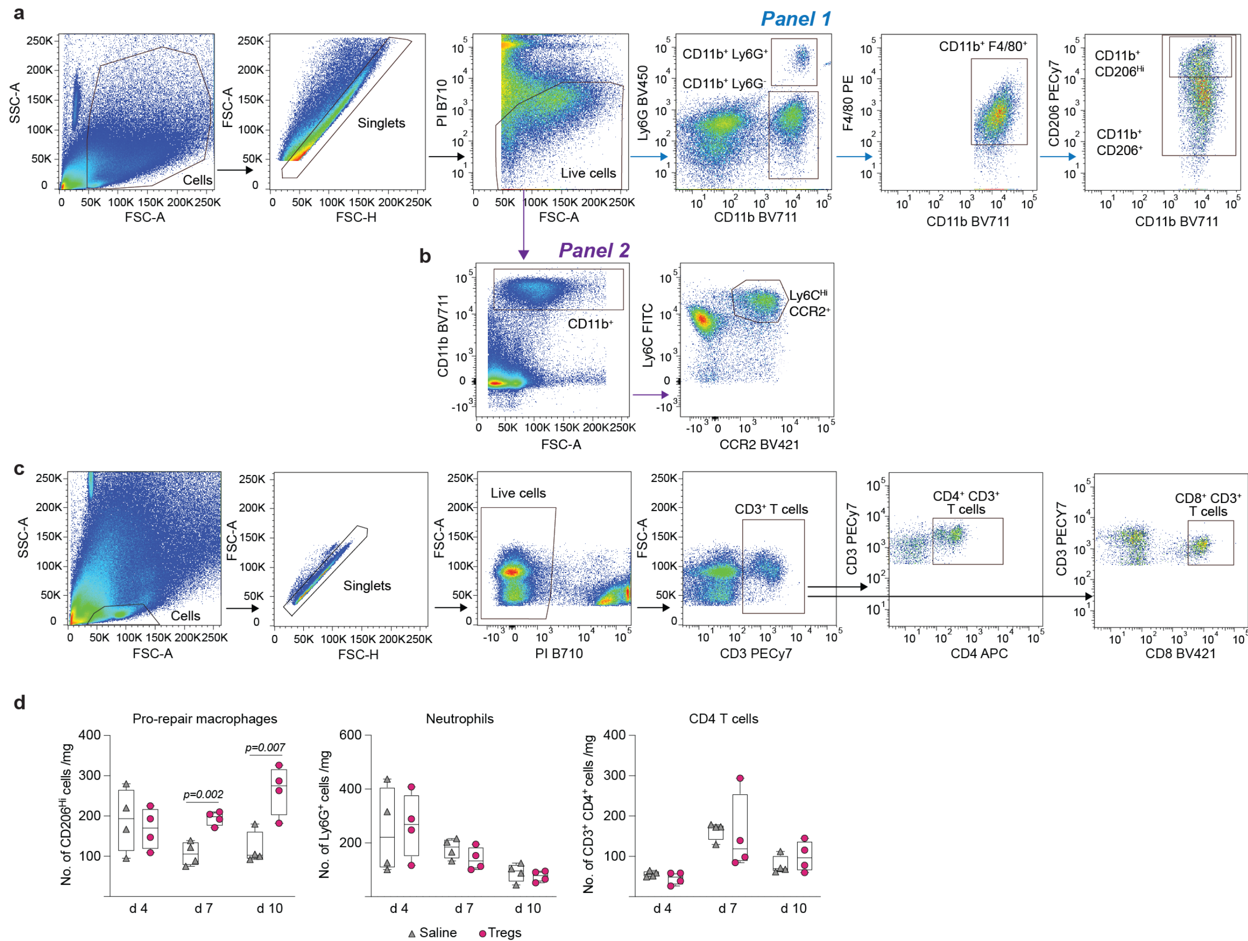

Supplementary Fig. 10 | Profiling of immune cell populations in the infarct zone. a-d. Mice received saline or Tregs one day after MI, and the immune cells in the infarct zone were analysed by flow cytometry. **a, b.** Flow cytometry plots representing the step-by-step gating strategy to analyse neutrophils and Mo/MΦ. Neutrophils ($CD11b^+$ $Ly6G^+$) were gated from total live cells. Cells were split in two panels, panel 1 included: Total Mo/MΦ ($CD11b^+$ $F480^+$) were gated from $CD11b^+$ $Ly6G^–$ cells. Pro-repair Mo/MΦ ($CD206^+$) were gated from $CD11b^+$ $F4/80^+$ cells. $CD206^{Hi}$ was gated from the total $CD206^+$ population. Panel 2 in (**b**) included: Mo/MΦ ($CD11b^+$) were gated from live cells, and the $Ly6C^{Hi}$ $CCR2^+$ population was gated subsequently. **c.** Flow cytometry plots representing the step-by-step gating strategy to analyse T cells. Total $CD3^+$ T cells were gated from live cells, and $CD8^+$ and $CD4^+$ T cells were gated from $CD3^+$ T cells. **d.** Number (No.) of pro-repair Mo/MΦs ($CD206^{Hi}$), neutrophils ($CD11b^+$, $Ly6G^+$), and $CD4^+$ $CD3^+$ T cells per mg of tissue (n=4). For all graphs, boxes show median (centre line) and interquartile range (edges), whiskers show the range of values and dots represent individual data points. Two-way ANOVA with Bonferroni *post-hoc* test for pair-wise comparisons was used to compare the groups in (**d**). *P* values are indicated.

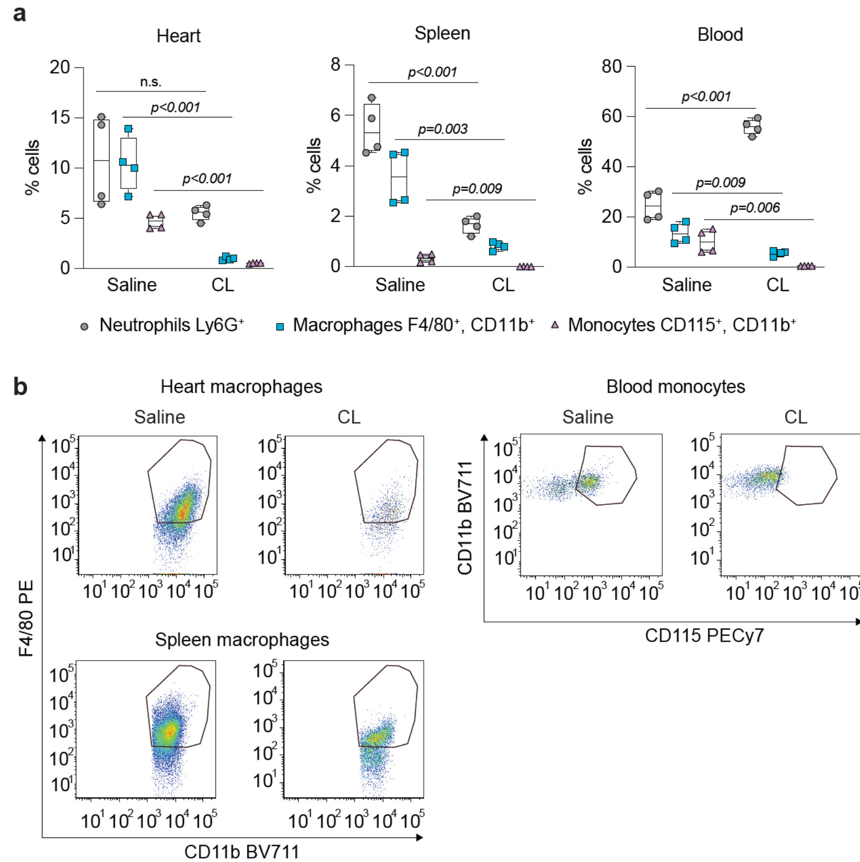

Supplementary Fig. 11 | Evidence of Mo/MΦ depletion with clodronate liposomes. **a, b.** Mice received saline control or clodronate liposomes (CL) via intraperitoneal injection starting one day before injury, on day of surgery and every second day until day 6. **a.** On day 4 post MI, myeloid populations were analysed in the heart, blood, and spleen. For all graphs, boxes show median (centre line) and interquartile range (edges), whiskers show the range of values and dots represent individual data points (n=4). **b.** Representative flow cytometry plots of the Mo/MΦ population in the heart, spleen and blood. Two-way ANOVA with Bonferroni *post-hoc* test for pair-wise comparisons was used to compare the groups in (**a**). *P* values are indicated.

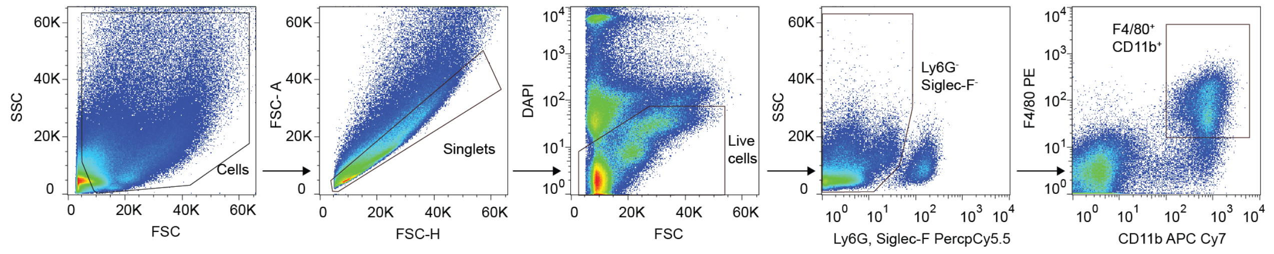

Supplementary Fig. 12 | Sorting strategy of Mo/MΦs. Flow cytometry plots representing the step-by-step gating strategy to sort total Mo/MΦs (CD11b$^+$, F480$^+$) on day 4 and 7 post-MI. Mo/MΦs (CD11b$^+$, F480$^+$) were gated by excluding the neutrophil (Ly6G) and eosinophil (Siglec-F) populations.

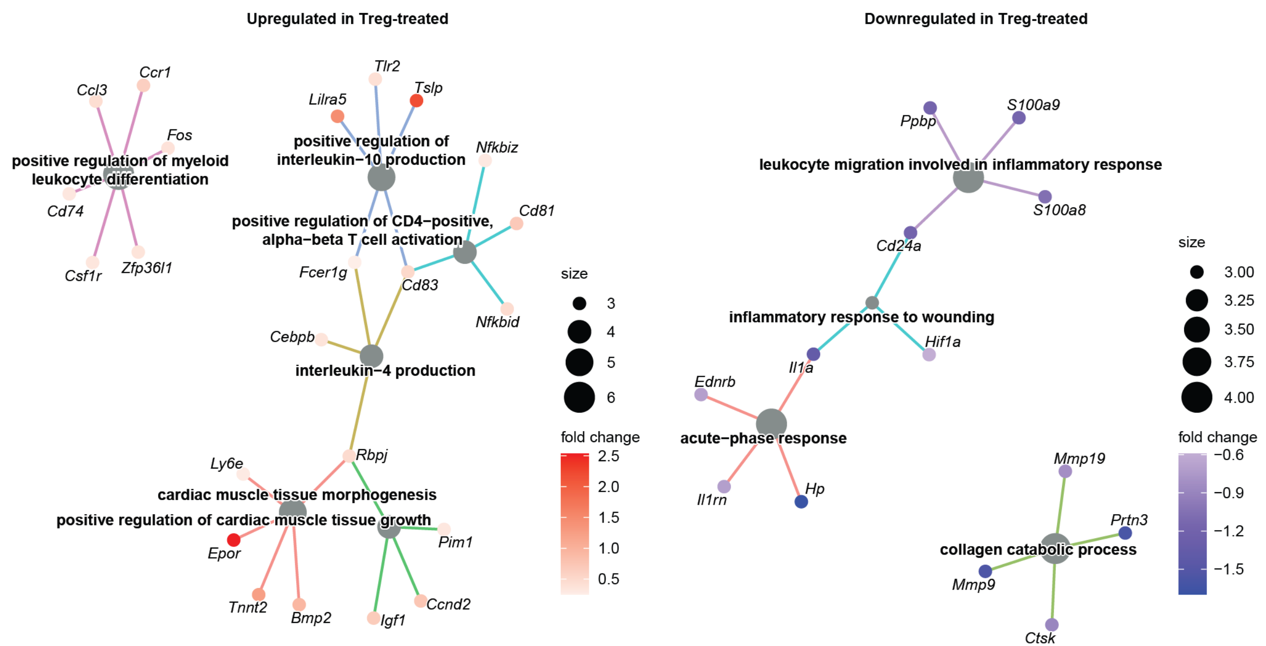

Supplementary Fig. 13 | Gene-concept network plot of top GO processes enriched in infract zone Mo/MΦ from Treg-treated mice. Network of the top GO biological processes (with adjusted $P < 0.01$; Bonferroni correction) enriched in the differentially expressed Mo/MΦ genes combined from both day 4 and day 7 post-MI in Treg-treated mice. The circle size represents the number of genes associated with the term and fold change indicates expression levels with red colour depicting upregulation and blue colour representing downregulation. The individual colours of the lines within the gene network depict individual GO terms.

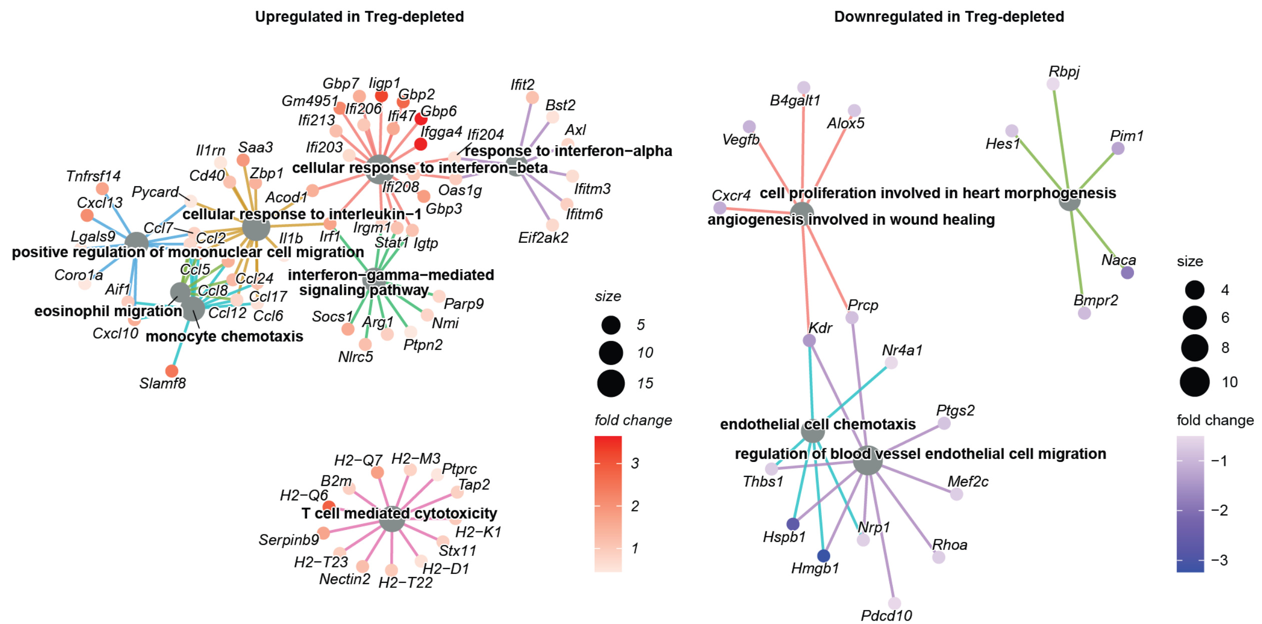

Supplementary Fig. 14 | Gene-concept network plot of top GO processes enriched in infract zone Mo/MΦ from Treg-depleted mice. Network of the top GO biological processes (with adjusted $P < 0.01$; Bonferroni correction) enriched in the differentially expressed Mo/MΦ genes combined from both day 4 and day 7 post-MI in Treg-depleted mice. The circle size represents the number of genes associated with the term and fold change indicates expression levels with red colour depicting upregulation and blue colour representing downregulation. The individual colours of the lines within the gene network depict individual GO terms.

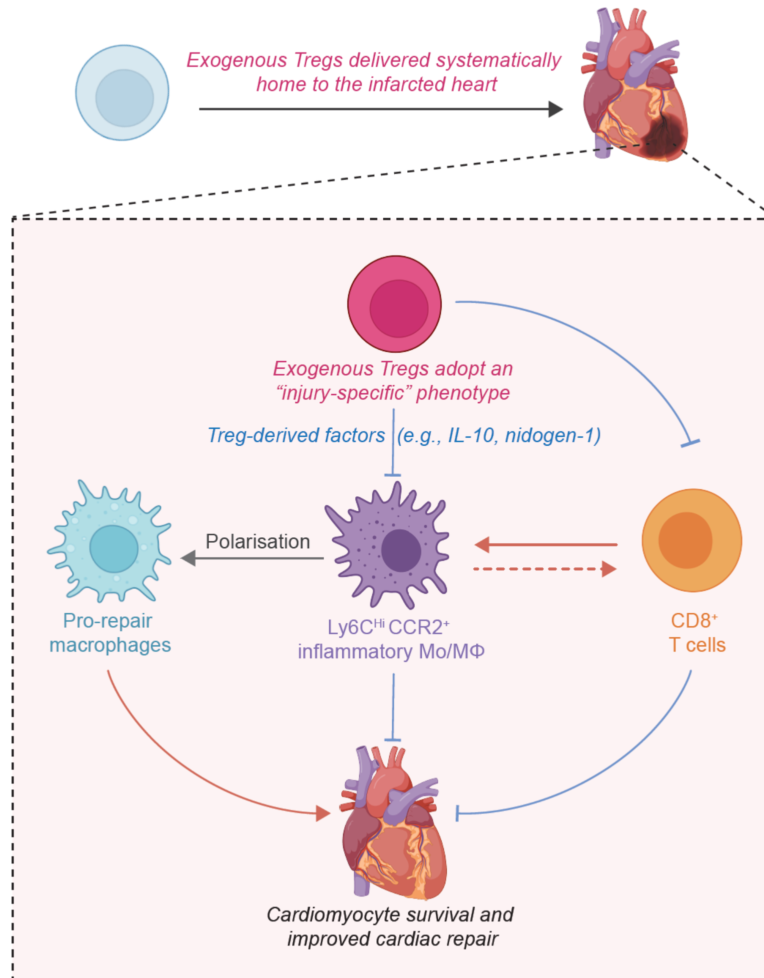

Supplementary Fig. 15 | Overall mechanisms by which exogenous Tregs improve cardiac repair post-MI. Tregs delivered systemically home to the heart and adopt an injury-specific phenotype. The delivered Tregs rapidly regulate immune cells in the infarct zone post-MI by reducing the number of Ly6C^{Hi} CCR2^{+} inflammatory Mo/MΦ and cytotoxic CD8^{+} T cells. The reduction of Ly6C^{Hi} CCR2^{+} Mo/MΦ is likely due to a direct effect via exogenous Treg-derived factors nidogen-1 and IL-10, as well as an indirect consequence of the lower CD8^{+} T cell number. As a result, Mo/MΦ rapidly transition to an anti-inflammatory and pro-repair phenotype. The fast modulation of the immune response is likely to be the main contributor to improved survival of cardiomyocytes, leading to an overall improved cardiac function. Red arrows indicate induction and blue arrows indicate inhibition. The dotted arrow is a hypothesised mechanism by which Ly6C^{Hi} CCR2^{+} Mo/MΦ influences the accumulation of CD8^{+} T cells. The black arrow indicates polarisation of Ly6C^{Hi} CCR2^{+} Mo/MΦ to a pro-repair macrophage subset. Figure created with BioRender.com released under a Creative Commons Attribution-NonCommercial-NoDerivs 4.0 International license (https://creativecommons.org/licenses/by-nc-nd/4.0/deed.en).